J|A|C|S
COMMUNICATIONS

Sulfur K-Edge XAS as a Probe of Sulfur-Centered Radical Intermediates

Vlad Martin-Diaconescu and Pierre Kennepohl*

The University of British Columbia, Department of Chemistry, Vancouver BC V6T 1Z1

Received October 26, 2006; E-mail: pierre@chem.ubc.ca

The redox chemistry of sulfur-containing amino acids has garnered significant attention in recent years. Particularly, cysteinyl-based (thiyl) radical intermediates have been proposed and implicated in various biological reactions[1] including, most prominently, the catalytic reduction of ribose sugars in ribonucleotide reductases.[2,3] At times, such intermediates have proven challenging to detect and quantify in situ using commonly available spectroscopic tools. The most direct approach to radical detection is electron paramagnetic resonance (EPR) spectroscopy, which can provide a wealth of information about unpaired electrons and their coupling with surrounding nuclei. However, the relatively large spin−orbit coupling parameter of sulfur ($\xi = 382\ \mathrm{cm}^{-1}$)[4] and resultant broad signal for the $g_{\|}$ component of thiyl ($\mathrm{RS}^{\bullet}$) radicals[5,6] decreases its sensitivity significantly such that other spectroscopic approaches may provide new opportunities for detection and characterization of this emerging class of biologically relevant redox-active moieties.

We have explored the use of X-ray absorption spectroscopy (XAS) at the sulfur K-edge as a complementary approach to the spectroscopic characterization of sulfur-centered radicals. In contrast to EPR, this approach provides the benefits of element-specificity as well as the ability to detect and characterize EPR-silent intermediates. This type of approach has been used to evaluate metal−ligand bonding in sulfur-coordinated species and has recently provided insights into the electronic structure of certain metal-coordinated ligand radical species.[7,8] Its applicability toward identification of free radicals has not been demonstrated, and we now provide the first example of direct XAS detection of isolated free radicals.

Glutathione (GSH) is a cysteine-containing tripeptide involved in biological redox buffering via a redox equilibrium between its reduced monomeric form and its two-electron oxidized dimeric form, that is, $2\mathrm{GSH} \rightleftharpoons \mathrm{GSSH} + 2\mathrm{e}^-$. It has also been shown that photochemical one-electron oxidation of GSH forms several radical products including the short-lived thiyl ($\mathrm{GS}^{\bullet}$) and long-lived perthiyl ($\mathrm{GSS}^{\bullet}$) radicals. Details of the one-electron redox chemistry of GSH are still somewhat unclear and deserve greater study. We have therefore utilized polycrystalline GSH as a prototype system for evaluating the use of S K-edge XAS in the study of sulfur-containing radicals in biochemically relevant species.

UV irradiation of polycrystalline GSH with a Spectroline UV lamp ($\lambda = 254$ nm) at room temp (295 ± 5 K) produces a complex EPR spectrum (see Supporting Information, Figure S1) that has been attributed to a mixture of radical species (i.e., $\mathrm{GS}^{\bullet}$, $\mathrm{G}^{\bullet}$, $\mathrm{H}^{\bullet}$, and $\mathrm{GSS}^{\bullet}$).[3] Samples were irradiated (0.5 to 48 h) and mounted as a finely ground powder dusted on sulfur-free Kapton tape for S K-edge XAS data collection. EPR of the UV-irradiated samples remained unchanged even after prolonged exposure to the X-ray beam (>3 h) and were not affected by the Kapton tape.

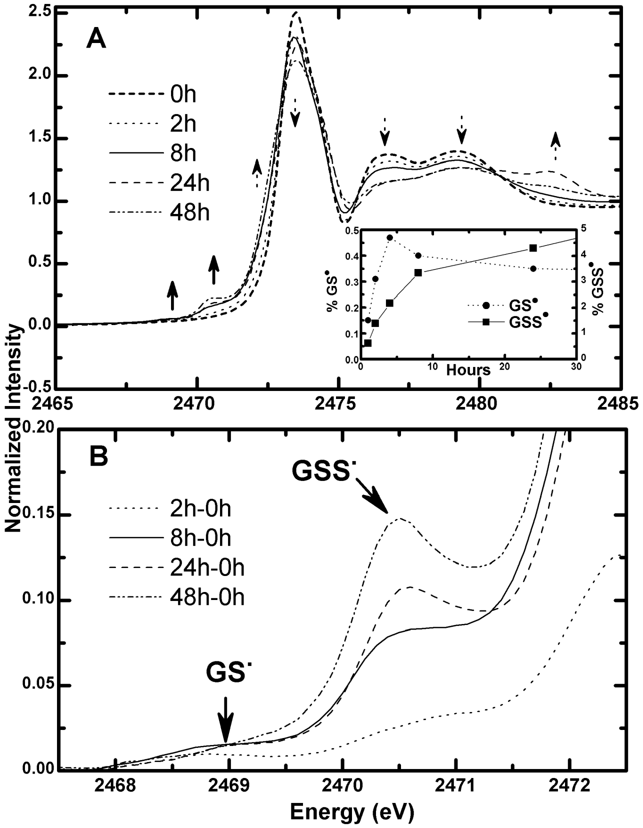

Figure 1. S K-edge XAS spectra of UV-irradiated GSH: (A) spectra of UV-irradiated GSH samples (inset shows estimated radical yields, see text and S3 for details) and (B) pre-edge spectra of UV-irradiated GSH after subtraction of GSH standard.

The S K-edge data (Figure 1A) show marked changes both below and above the ionization edge. The GSH spectrum is dominated by an intense $\mathrm{CS}_{\sigma^*} \leftarrow \mathrm{S}_{1s}$ at ∼2473.5 eV.[9] Upon UV-irradiation, new pre-edge features appear at 2468.8 ± 0.3 and 2470.5 ± 0.3 eV as the $\mathrm{CS}_{\sigma^*} \leftarrow \mathrm{S}_{1s}$ feature of GSH broadens and decreases in intensity. A third feature is also observed in the second derivative of the data at 2471.5 ± 0.4 eV (see Figure S2). These low-energy pre-edge features coincide with the appearance of radical species in the EPR spectra and thus should correspond to transitions to the half-occupied sulfur valence orbitals of sulfur-centered free radicals. Principal component analysis[10] indicates that only two kinetically distinct species are required to fit the pre-edge data in addition to the GSH starting material (Figure 1A inset and Supporting Information, section S7). The electronic nature of these transitions was probed using a combination of unrestricted ground state and time-dependent density functional theory (TDDFT) calculations on simplified models of potential thiyl and perthiyl radicals.

Electron density maps of the important empty valence orbitals are given in Figure 2. Since transitions at the S K-edge are dominated by the electric dipole allowed $\mathrm{S}_{3p} \leftarrow \mathrm{S}_{1s}$ component, valence orbitals with S_{3p} character are of greatest significance. On the basis of the DFT results,[11−13] the unpaired electron in $\mathrm{GS}^{\bullet}$ should reside in a singly occupied S_{3p} orbital perpendicular to the S−C bond axis.[6] Transitions to two other orbitals (CS_{σ^*} and HC_{σ^*})

10.1021/ja0676760 CCC: $37.00

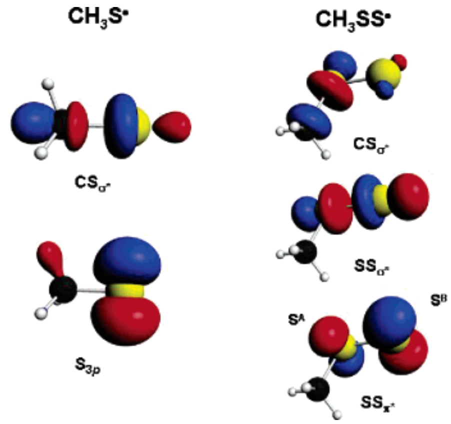

Figure 2. Electron density contour maps of important low-lying valence orbitals, as calculated by DFT (isovalue = 0.075 e·Å^{-3}).

Table 1. Sulfur K-Edge Pre-edge Features of Relevant Model Compounds As Calculated Using TDDFT

species	assignment	energy (eV)	f
CH_3SH	$CS_{\sigma*} + HS_{\sigma*} \leftarrow S_{1s}$	2472.8	2.0×10^{-3}
	$CS_{\sigma*} \leftarrow S_{1s}$	2473.7	1.1×10^{-3}
	$CS_{\sigma*} + HS_{\sigma*} \leftarrow S_{1s}$	2474.4	1.3×10^{-3}
$CH_3S^•$	$S_{3p} \leftarrow S_{1s}$	2468.8	3.9×10^{-3}
	$HC_{\sigma*} \leftarrow S_{1s}$	2473.7	8.1×10^{-4}
	$CS_{\sigma*} \leftarrow S_{1s}$	2474.5	9.3×10^{-4}
$CH_3SS^•$	$SS_{\pi*} \leftarrow S^B{}_{1s}$	2469.3	2.5×10^{-3}
	$SS_{\pi*} \leftarrow S^A{}_{1s}$	2470.6	1.8×10^{-3}
	$SS_{\sigma*} \leftarrow S^B{}_{1s}$	2472.7	3.1×10^{-3}
	$CS_{\sigma*} \leftarrow S^B{}_{1s}$	2473.4	5.3×10^{-4}
	$SS_{\sigma*} \leftarrow S^A{}_{1s}$	2474.1	2.6×10^{-3}
	$CS_{\sigma*} \leftarrow S^A{}_{1s}$	2474.8	1.6×10^{-3}

containing significant S_{3p} character yield an edge feature at ∼2474 eV corresponding to σ* contributions.[14] The transition to the nearly pure (∼92%) singly occupied S_{3p} orbital results in a strong pre-edge feature ∼5 eV lower in energy (see Table 1).

The unpaired electron in GSS$^•$ is located in a $SS_{\pi*}$ orbital (Figure 2); two transitions to this orbital should be observed, one from each of the S_{1s} orbitals. TDDFT calculations indicate a significant splitting of the two $SS_{\pi*}$ transitions (1.3 eV) resulting from greater oxidation of S^A, which lowers its S_{1s} orbital energy. The σ* manifold for GSS$^•$ includes both $CS_{\sigma*}$ and $SS_{\sigma*}$ contributions and occurs at about the same energy as in GSH. Importantly, the pre-edge feature for GSS$^•$ should occur at higher energy than that of GS$^•$, owing to the antibonding nature of the acceptor orbital in GSS$^•$. In addition, one would expect a splitting of the pre-edge feature in GSS$^•$ caused by differences in Z_{eff} for the two S atoms.

The calculated electronic structures and core excitation spectra are in good agreement with the experimental S K-edge data. The lowest energy pre-edge feature corresponds to a $S_{3p} \leftarrow S_{1s}$ transition in GS$^•$, whereas the higher-energy split feature that grows in subsequently corresponds to transitions to the $SS_{\pi*}$ of GSS$^•$. The observed splitting and intensity ratio are similar to that predicted by DFT. The kinetic behavior of the S K-edge pre-edge features are also consistent with previously published EPR data, showing initial formation of the thiyl radical followed by subsequent formation of the longer-lived perthiyl species.[3] At much longer times, we note the presence of a higher-energy feature (2482.6 eV), corresponding to a highly oxidized sulfur species. We have, as yet, not identified the species responsible for this feature although the formation of stable sulfoxyl radicals has been reported upon photooxidation of cysteine side chains.[3]

This study provides the first example of direct detection and characterization of isolated free radicals using XAS. Importantly, pre-edge features of the different radical species are well resolved from the intense σ* contributions, thus such data can provide useful complementary information in the investigation of radical intermediates. Furthermore, we note that the $g_{||}$ of GS$^•$ is *not* observed under these experimental conditions, whereas the S K-edge pre-edge feature is clearly discernible. Our ability to investigate the one-electron chemistry of sulfur-containing amino acids will be significantly improved with the availability of this new approach. S K-edge XAS has been an untapped resource for the investigation of these species, and our initial studies suggest it should provide unique insights into the redox chemistry of sulfur-containing amino acids and their biological implications.

Acknowledgment. This research is funded by NSERC (Canada). EPR data were obtained at the UBC Paramagnetic Research Lab, funded in part by the Canada Foundation for Innovation (CFI) and the British Columbia Knowledge Development Fund (BCKDF). Startup funds and infrastructure support provided by UBC. Special thanks to Dr. Serena DeBeer George at the Stanford Synchrotron Radiation Laboratory (SSRL) for technical and scientific assistance during data collection. Portions of this research were carried out at SSRL, a national user facility operated by Stanford University on behalf of the U.S. DOE-BES. The SSRL Structural Molecular Biology Program is supported by DOE, Office of Biological and Environmental Research, and by the NIH, National Center for Research Resources, Biomedical Technology Program.

Supporting Information Available: EPR spectra (Figure S1), second derivative XAS spectra (Figure S2), radical yield analysis (Figure S3), DFT input files (sections S4−S6), and experimental details (section S7). This material is available free of charge via the Internet at http://pubs.acs.org.

References

(1) Giles, N. M.; Giles, G. I.; Jacob, C. *Biochem. Biophys. Res. Commun*. **2003**, *300*, 1−4.
(2) Silva, D. J.; Stubbe, J.; Samano, V.; Robins, M. *J. Biochemistry* **1998**, *37*, 5528−5535.
(3) Lassmann, G.; Kolberg, M.; Bleifuss, G.; Graslund, A.; Sjoberg, B. M.; Lubitz, W. *Phys. Chem. Chem. Phys.* **2003**, *5*, 2442−2453.
(4) Carrington, A.; McLachlan, D. M. *Introduction to Magnetic Resonance*; Harper & Row: New York, 1969.
(5) Symons, M. C. R. *J. Chem. Soc., Perkin Trans. 2* **1974**, 1618−1620.
(6) van Gastel, M.; Lubitz, W.; Lassmann, G.; Neese, F. *J. Am. Chem. Soc.* **2004**, *126*, 2237−2246.
(7) Szilagyi, R. K.; Lim, B. S.; Glaser, T.; Holm, R. H.; Hedman, B.; Hodgson, K. O.; Solomon, E. I. *J. Am. Chem. Soc.* **2003**, *125*, 9158−9169.
(8) Szilagyi, R. K.; Frank, P.; George, S. D.; Hedman, B.; Hodgson, K. O. *Inorg. Chem.* **2004**, *43*, 8318−8329.
(9) Rompel, A.; Cinco, R. M.; Latimer, M. J.; McDermott, A. E.; Guiles, R. D.; Quintanlha, A.; Krauss, R. M.; Sauer, K.; Yachandra, V. K.; Klein, M. P. *Proc. Natl. Acad. Sci. U.S.A.* **1998**, *95*, 6122−6127.
(10) Webb, S. M. *Phys. Scr.* **2005**, *T115*, 1011−1014.
(11) Velde, G. T.; Bickelhaupt, F. M.; Baerends, E. J.; Guerra, C. F.; Van, Gisbergen, S. J. A.; Snijders, J. G.; Ziegler, T. *J. Comput. Chem.* **2001**, *22*, 931−967.
(12) Guerra, C. F.; Snijders, J. G.; Velde, G. T.; Baerends, E. *J. Theor. Chem. Acc.* **1998**, *99*, 391.
(13) ADF2005.01, SCM, Theoretical Chemistry, Vrije Universiteit, Amsterdam, The Netherlands, http://www.scm.com.
(14) The $HC_{\sigma*}$ final state obtains much of its S K-edge intensity through intensity borrowing from the $CS_{\sigma*}$ state at ∼1 eV higher energy.

JA0676760